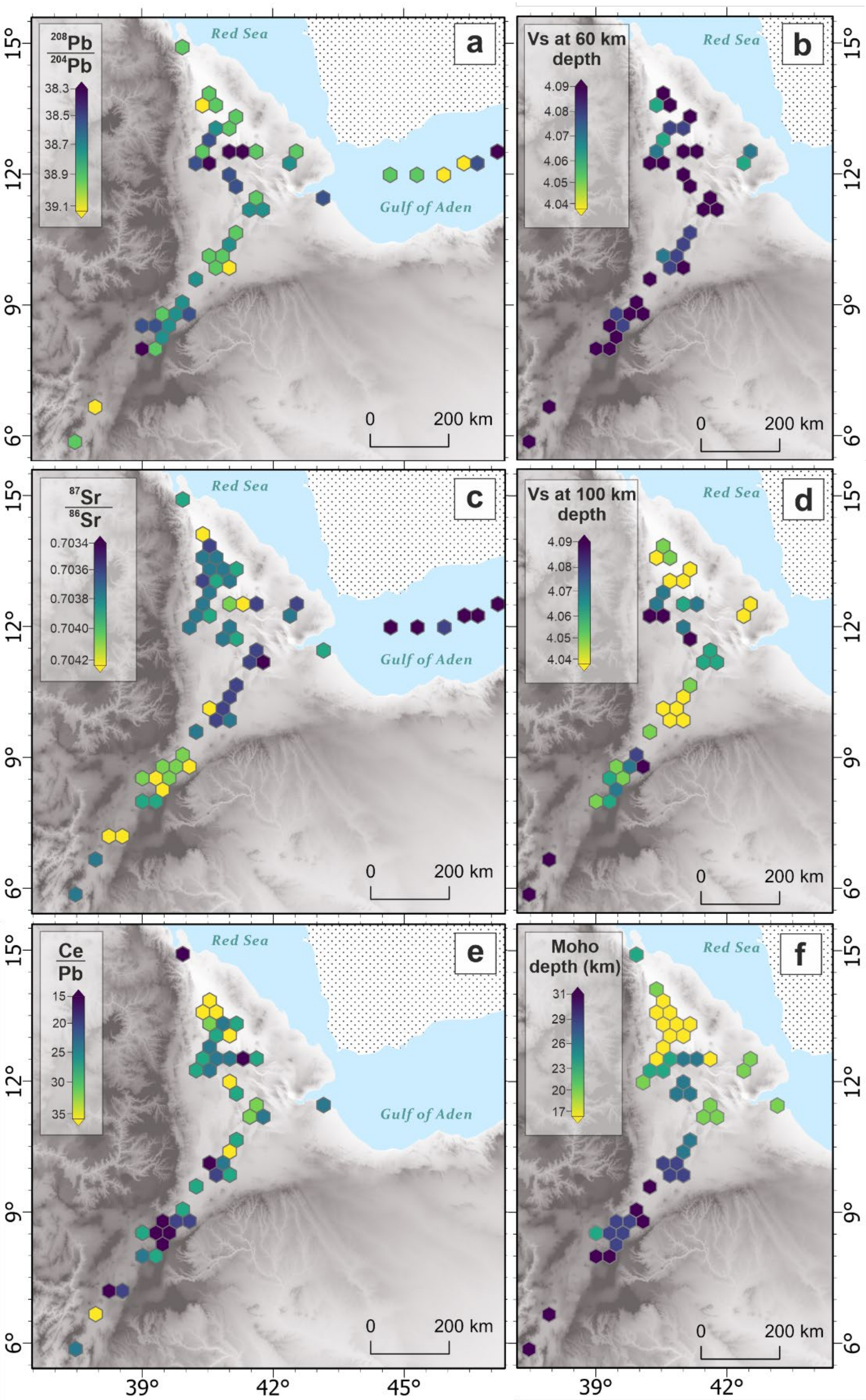

Extended Fig. 1 Hex maps showing the patterns for the selected variables (see Section 1 for further details) across the study region. (a) $^{208}Pb/^{204}Pb$; (b) Shear wave velocity (Vs) at 60 km; (c) $^{87}Sr/^{86}Sr$; (d) Shear wave velocity (Vs) at 100 km; (e) Ce/Pb; (f) Moho depth (km).

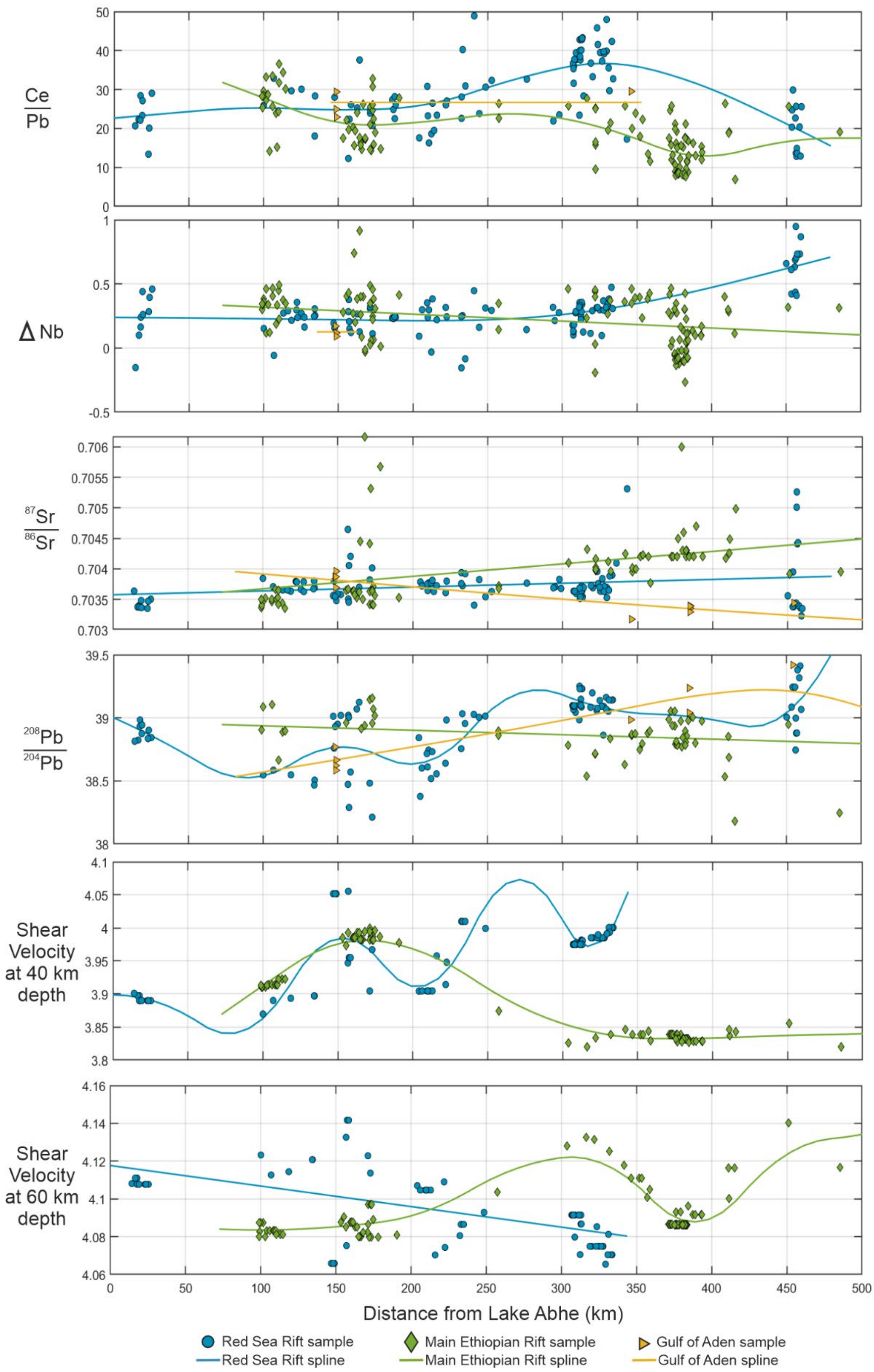

Extended Fig. 2 Splines (lines) of the winning model (C1C) for remaining selected variables not shown in Figure 3. Symbols show the data within the study (blue circles = Red Sea Rift, green diamonds = Main Ethiopian Rift, yellow triangles = Gulf of Aden Rift).

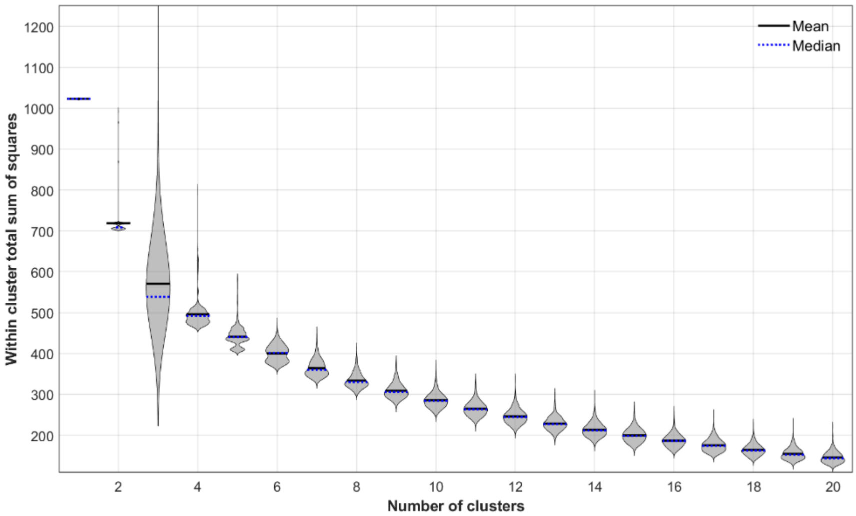

Extended Fig. 3 (a) Violin plot showing the within cluster sum of squares for the k–means cluster analysis testing number of clusters between 1 and 20, for 1000 iterations.

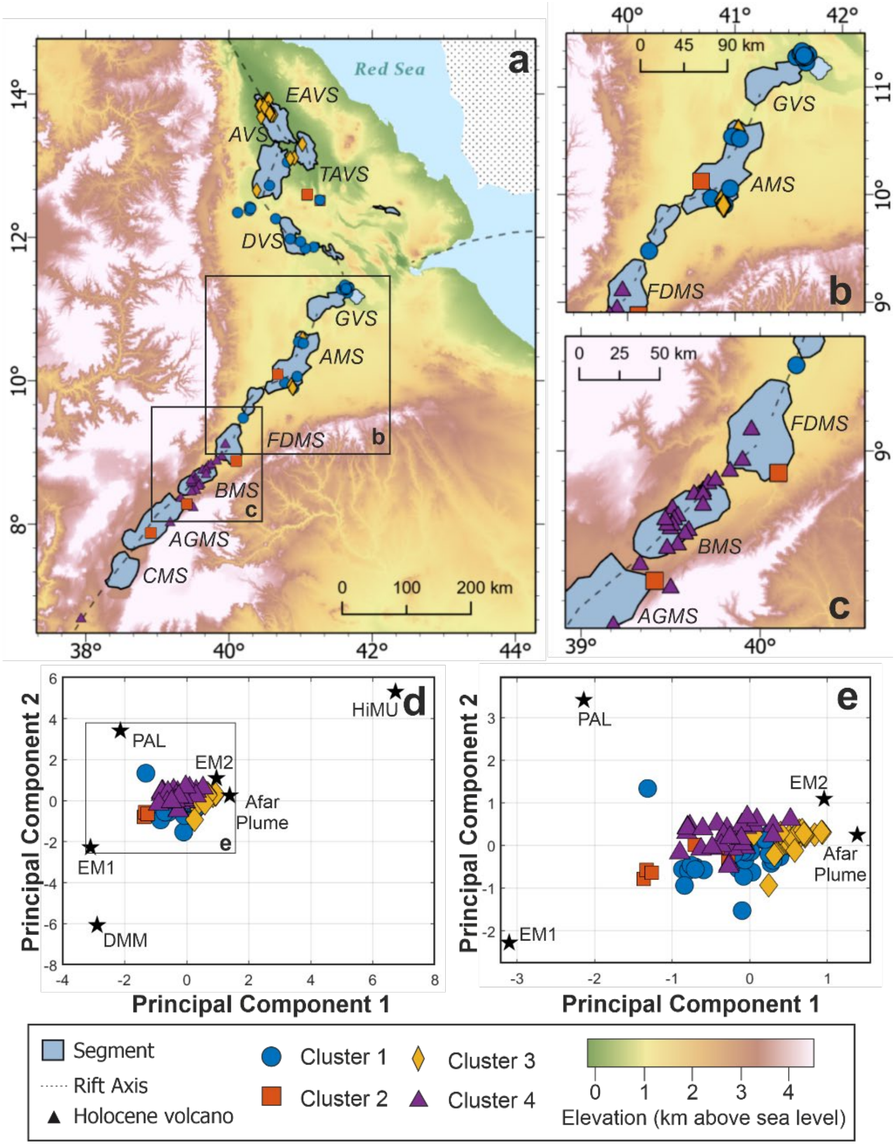

Extended Fig. 4 Map of the segments and cluster assignment (see legend) within the study region. Segments are shown in blue from north to south: Erta Ale Volcanic Segment (EAVS), Tat'Ale Volcanic Segment (TAVS), Alayta Volcanic Segment (AVS), Dabbahu Volcanic Segment (DVS), Gabillema Volcanic Segment (GVS), Adda'do Magmatic Segment (AMS), Fentale-Dofen Magmatic Segment (FDMS), Boset Magmatic Segment (BMS), Aluto-Gedamsa Magmatic Segment (AGMS), Corbetti Magmatic Segment (CMS). Rift axis (dotted line) and Holocene volcanoes (black triangles) are shown. (b) and (c) are enlarged maps of the boxes shown in (a). (d) & (e) Principal component analysis bi-plot (PC1 vs PC2) when considering the six isotopic systems (see Section 1) showing the samples and their component scores relative to those of the mantle end- members.

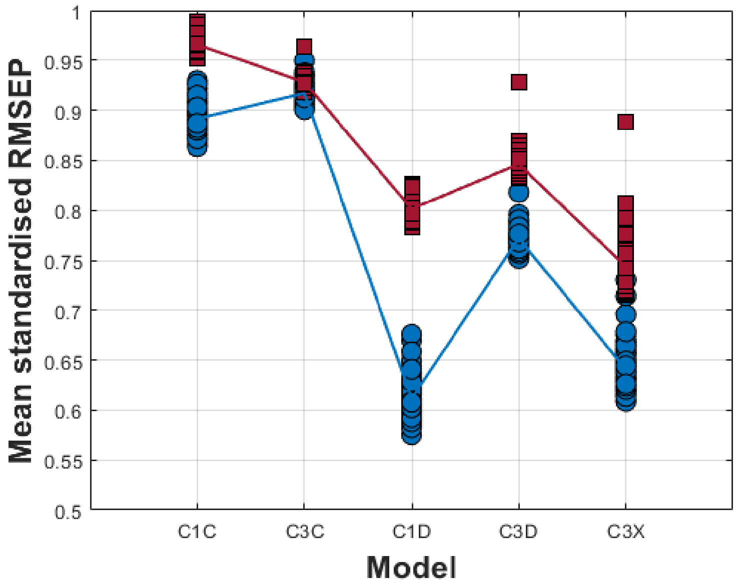

Extended Fig. 5 The mean standardised root means square error of prediction (RMSEP) for each of the models tested (described in Section 5.5) when excluding any observations that have a Ce/Pb > 20. Individual linear model results are shown by red squares and the mean of those results are displayed by the red line. Individual spline results are shown by blue circles and the mean of those results are shown by a blue line.

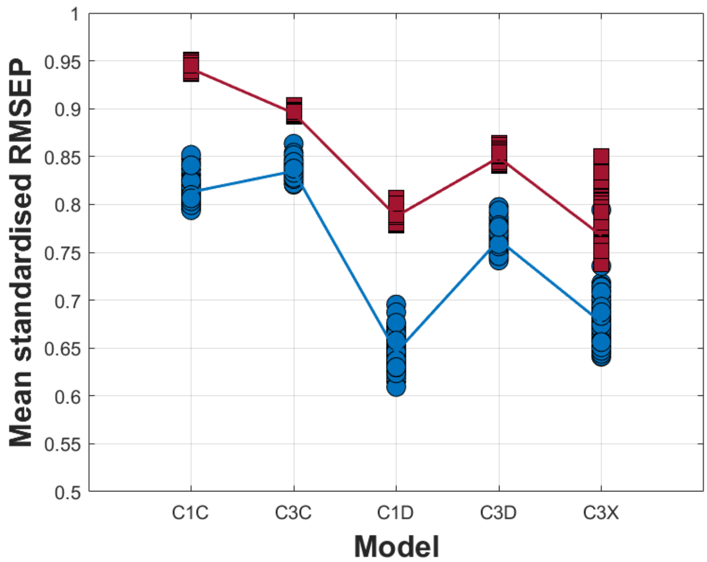

Extended Fig. 6 The mean standardised root means square error of prediction (RMSEP) for each of the models tested (described in Section 5.5) when excluding the Gulf of Aden. Key is as shown in Extended Fig. A6.

Model	Description
C1C	A singular upwelling centred at Lake Abhe (11.192 ◦N 41.784 ◦E) with each rift (i.e., Red Sea Rift, Gulf of Aden rift and Main Ethiopian Rift) behaving the same (not independent), based on the theory of [5]. This model fits a single line using all the data points from each rift.
C3C	Three upwellings centred at Lake Abhe (11.192 ◦N 41.784 ◦E), and two other points across the region (14.008 ◦N 40.458 ◦E & 6.626 ◦N 37.948 ◦E); a model based on the locations of previously proposed small-scale upwelling locations through numerical modelling [30]. Assumes each rift behaves the same (not independent of each other) and the upwellings are of the same composition. This model fits a single line across all the data points
C1D	A singular upwelling centred at Lake Abhe (11.192 ◦N 41.784 ◦E) with each rift behaving independently. This model fits three lines (one for each rift) across the data points for the corresponding rift
C3D	Three small-scale upwellings centred at Lake Abhe (11.192 ◦N 41.784 ◦E), and two other points across the region (14.008 ◦N 40.458 ◦E & 6.626 ◦N 37.948◦E) with each rift acting independently. This model assumes each upwelling is compositionally the same and fits three lines (one for each rift) across the data points for the corresponding rift
C3X	Three small-scale upwellings centred at Lake Abhe (11.192 ◦N 41.784 ◦E), and two other points across the region (14.008 ◦N 40.458 ◦E & 6.626 ◦N 37.948 ◦E) with each rift and upwelling acting independently. This model plots five lines.

Extended Table 1: Models considered when assessing the Afar upwelling characteristics. Details of each model are described.

Variable (s)	**Observed Range**	**Details**
^{206}Pb/^{204}Pb	17.853 to 19.608	^{206}Pb/^{204}Pb >20 is linked to HIMU, ^{206}Pb/^{204}Pb ranging from 19.2 to 20.5 indicates a mantle upwelling source (C, FOZO) [73] and ^{206}Pb/^{204}Pb <17.8 can be related to a depleted mantle component 74].
^{207}Pb/^{204}Pb	15.448 to 15.697	^{207}Pb/^{204}Pb <15.5 is related to a depleted mantle component [74], ^{207}Pb/^{204}Pb >15.65 is linked to the HiMU component and ^{207}Pb/^{204}Pb ~ 15.6 indicates a mantle upwelling source (C, FOZO). A ^{207}Pb/^{204}Pb >15.75 is linked to crustal values [16, 36].
^{208}Pb/^{204}Pb	37.984 to 39.420	^{208}Pb/^{204}Pb <38 is related to a depleted mantle component [2], ^{208}Pb/^{204}Pb >39.5 is linked to the HiMU component and ^{208}Pb/^{204}Pb 39.2 to 39.5 indicates a mantle upwelling source (C, FOZO). A ^{208}Pb/^{204}Pb >39.7 is linked to crustal values [16, 36].
^{143}Nd/^{144}Nd	0.51259 to 0.51317	A low ^{143}Nd/^{144}Nd (<0.5121) indicates continental crust or Pan African Lithosphere. ^{143}Nd/^{144}Nd values ~ 0.51285 indicates a HIMU or upwelling related mantle source. Higher ^{143}Nd/^{144}Nd values (>0.5131) indicate a depleted mantle source (i.e., DMM) [24, 73, 75].
^{87}Sr/^{86}Sr	0.70280 to 0.70678	A low 87Sr/86Sr (0.7040-0.7045) indicates a mantle component that is either depleted (DMM) or an upwelling (HIMU, C). A higher ^{87}Sr/^{86}Sr (<0.705) indicates the potential influence from continental crust [24, 73, 75].
Ce/Pb	6.84 to 48.92	A Ce/Pb >30 is commonly attributed to a recycled mantle source that has been depleted in fluid mobile elements (i.e., Pb, Ba, Sr, K) during subduction, therefore resulting in high fluid-immobile-element to fluid-mobile -element ratios (i.e., Ce/Pb). Typical mantle has a Ce/Pb value of 25±5 and crust a value of ~4 [35].
La/Sm	0.4 to 4.7	(La/Sm) >1 indicates LREE enrichment fractionation (alkali basalts or upwelling), (La/Sm) <1 indicates LREE depleted (mid-ocean ridge). The higher the La/Sm the lower the melt fraction [5]
ΔNb	-0.26 to 0.95	Differentiates between a depleted mantle (ΔNb <0) and a mantle upwelling (ΔNb >0) [25].
Vs @ 40 km	3.81 to 4.06	Shear wave velocities can be sensitive, temperature, grainsize and the presence of fluids. A reduction in Vs can indicate a change in mantle composition or an increased proportion of melt/hydrothermal fluid [29]. This is the velocity from 40 km depth.
Vs @ 60 km	4.06 to 4.18	
Vs @ 80 km	4.00 to 4.16	
Vs @ 100 km	3.97 to 4.10	
Vs @ 120 km	4.03 to 4.10	

Extended Table 2: Variables used within the analysis summarising the ranges observed and why they have been selected.

	JA-2 (Imai et al., 1995), n=6					BCR-2 (Wilson., 1997), n=4					JB-2 (GeoREM), n=3					
	Mean	**Std.Dev**	**%RSD**	**Ref.**	**Uncert.**	**Mean**	**Std.Dev**	**%RSD**	**Ref.**	**Uncert.**	**Mean**	**Std.Dev**	**%RSD**	**Ref.**	**Uncert.**	**Accuracy %**
Li	29.41	0.25	0.85	29.18	0.60	9.04	0.12	1.33	9.13	0.22	8.16	0.16	1.96	8.08	0.15	0.99
Sc	17.91	0.19	1.06	18.93	0.30	32.55	0.17	0.52	33.53	0.40	55.35	0.52	0.94	54.08	0.76	2.35
V	115.38	4.32	3.74	119.70	2.40	403.50	5.06	1.25	417.60	4.50	575.27	9.98	1.73	572.40	8.30	0.50
Cr	397.18	13.36	3.36	424.80	9.30	14.56	0.47	3.23	15.85	0.38	24.63	0.31	1.26	26.65	0.69	7.58
Co	27.55	0.20	0.73	28.33	1.00	36.86	0.19	0.52	37.33	0.37	37.18	0.58	1.56	37.57	0.67	1.04
Ni	127.20	1.68	1.32	136.00	2.20	11.72	0.41	3.50	12.57	0.30	13.65	0.29	2.12	14.77	0.51	7.58
Cu	30.36	0.97	3.19	29.00	1.50	23.06	1.24	5.38	19.66	0.72	222.63	2.76	1.24	222.10	3.60	0.24
Rb	72.17	1.29	1.79	69.80	1.30	46.46	0.92	1.98	46.02	0.56	6.24	0.25	4.01	6.40	0.11	2.50
Sr	245.67	1.43	0.58	245.80	3.00	333.78	1.47	0.44	337.40	6.70	175.90	2.21	1.26	178.20	1.50	1.29
Y	17.17	0.07	0.41	16.89	0.60	36.01	0.09	0.25	36.07	0.37	23.89	0.28	1.17	23.56	0.44	1.40
Zr	114.72	0.75	0.65	108.50	2.60	187.65	1.74	0.93	186.50	1.50	45.42	0.40	0.88	48.25	0.88	5.87
Nb	9.24	0.10	1.08	9.30	0.20	12.43	0.24	1.93	12.44	0.20	0.49	0.00	0.00	0.57	0.03	13.27
Cs	4.97	0.11	2.21	4.78	0.10	1.11	0.04	3.60	1.16	0.13	0.77	0.02	2.60	0.80	0.02	3.75
Ba	317.67	5.45	1.72	308.40	5.10	692.20	12.06	1.74	683.90	4.70	220.00	2.41	1.10	218.10	2.70	0.87
La	16.08	0.05	0.31	15.46	0.40	24.92	0.16	0.64	25.08	0.16	2.23	0.02	0.90	2.28	0.04	2.24
Ce	33.16	0.25	0.75	32.86	0.90	52.85	0.29	0.55	53.12	0.33	6.37	0.05	0.78	6.55	0.09	2.78
Pr	3.77	0.02	0.53	3.69	0.10	6.79	0.05	0.74	6.83	0.04	1.13	0.01	0.88	1.13	0.02	0.09
Nd	14.37	0.07	0.49	14.04	0.20	28.41	0.10	0.35	28.26	0.37	6.21	0.01	0.16	6.39	0.06	2.85
Sm	3.08	0.02	0.65	3.03	0.00	6.54	0.05	0.76	6.55	0.05	2.23	0.01	0.45	2.27	0.02	1.59
Eu	0.91	0.01	1.10	0.89	0.00	1.97	0.02	1.02	1.99	0.02	0.83	0.01	1.20	0.84	0.01	0.72
Gd	3.04	0.04	1.32	3.01	0.10	6.70	0.08	1.19	6.81	0.08	3.19	0.03	0.94	3.12	0.05	2.15
Tb	0.49	0.01	2.04	0.48	0.00	1.06	0.01	0.94	1.08	0.03	0.58	0.01	1.72	0.59	0.01	1.07
Dy	2.93	0.03	1.02	2.85	0.10	6.36	0.05	0.79	6.42	0.06	3.87	0.03	0.78	3.87	0.06	0.05
Ho	0.60	0.00	0.00	0.59	0.00	1.30	0.01	0.77	1.31	0.01	0.86	0.00	0.00	0.86	0.02	0.35
Er	1.72	0.02	1.16	1.68	0.00	3.62	0.05	1.38	3.67	0.04	2.51	0.03	1.20	2.54	0.04	1.06
Tm	0.26	0.00	0.00	0.25	0.00	0.53	0.01	1.89	0.53	0.01	0.38	0.01	2.63	0.39	0.01	3.31
Yb	1.68	0.02	1.19	1.65	0.00	3.39	0.04	1.18	3.39	0.04	2.52	0.01	0.40	2.53	0.03	0.36

	JA-2 (Imai et al., 1995), n=6					BCR-2 (Wilson., 1997), n=4					JB-2 (GeoREM), n=3					
	Mean	**Std.Dev**	**%RSD**	**Ref.**	**Uncert.**	**Mean**	**Std.Dev**	**%RSD**	**Ref.**	**Uncert.**	**Mean**	**Std.Dev**	**%RSD**	**Ref.**	**Uncert.**	**Accuracy %**
Lu	0.26	0.00	0.00	0.25	0.00	0.51	0.00	0.00	0.50	0.01	0.39	0.00	0.00	0.39	0.01	0.15
Hf	2.97	0.01	0.34	2.84	0.10	4.92	0.03	0.61	4.97	0.03	1.47	0.01	0.68	1.49	0.03	1.14
Ta	0.70	0.04	5.71	0.65	0.00	0.83	0.07	8.43	0.79	0.02	0.04	0.00	0.00	0.04	0.00	1.01
Pb	19.97	0.46	2.30	18.88	0.30	10.32	0.35	3.39	10.59	0.17	4.96	0.09	1.81	5.25	0.11	5.52
Th	4.92	0.07	1.42	4.80	0.10	5.81	0.12	2.07	5.83	0.05	0.26	0.02	7.69	0.26	0.00	0.93
U	2.28	0.04	1.75	2.18	0.10	1.67	0.04	2.40	1.68	0.02	0.15	0.00	0.00	0.15	0.00	1.83

Extended Table 3: Trace element averages of certified international reference materials summarised in [78]. Number of runs (n) for each reference material are shown.

End Member	**Afar Plume**	**Depleted Mantle**	**Pan African Lithosphere**	**HiMU**	**EMI**	**EMII**
$^{206}Pb/^{204}Pb$	19.5	17.5	17.85	22	17.4	19.3
$^{207}Pb/^{204}Pb$	15.6	15.3	15.75	15.84	15.48	15.64
$^{208}Pb/^{204}Pb$	39.2	36.6	39.75	40.75	39.0	39.75
$^{87}Sr/^{86}Sr$	0.512875	0.51335	0.5121	0.51285	0.51235	0.51235
$^{143}Nd/^{144}Nd$	0.7035	0.7022	0.7075	0.7025	0.7055	0.709
References	[36, 76]	[36,76]	[36, 77]	[76]	[76]	[76]

Extended Table 4: End member compositions used in the principal component analysis. References for values shown in the table.

End Member	**PC1**	**PC2**	**PC3**
$^{206}Pb/^{204}Pb$	0.3714	-0.5488	0.4249
$^{207}Pb/^{204}Pb$	0.5619	-0.1131	-0.5855
$^{208}Pb/^{204}Pb$	0.5727	-0.1835	0.1812
$^{87}Sr/^{86}Sr$	-0.3687	-0.5481	0.2860
$^{143}Nd/^{144}Nd$	0.2872	0.5933	0.6017
Variance explained (%)	53.15	37.42	5.01

Extended Table 5: Eigenvectors for the principal components 1-3 when principal component analysis is done on 5 radiogenic isotope variables. The amount of variance explained by each of the principal components is also included.

Extended Equation 1: Delta Niobium equation.

$$\Delta Nb = 1.74 + log\left(\frac{Nb}{Y}\right) - 1.92\ log\left(\frac{Zr}{Y}\right)$$